PHILOSOPHICAL TRANSACTIONS OF THE ROYAL SOCIETY A MATHEMATICAL, PHYSICAL & ENGINEERING SCIENCES

Near-Limiting Gravity Waves in Water of Finite Depth

J. M. Williams

Phil. Trans. R. Soc. Lond. A 1985 **314**, 353-377
doi: 10.1098/rsta.1985.0022

Phil. Trans. R. Soc. Lond. A **314**, 353–377 (1985) [353]
Printed in Great Britain

NEAR-LIMITING GRAVITY WAVES IN WATER OF FINITE DEPTH

By J. M. WILLIAMS†
Hydraulics Research Ltd, Wallingford, Oxfordshire OX10 8BA, U.K.

(*Communicated by F. Ursell, F.R.S.* – *Received* 17 *April* 1984)

CONTENTS

Progressive, irrotational gravity waves of constant form, with all crests in a wave train identical, exist as a two-parameter family. The first parameter, the ratio of mean depth to wavelength, varies from zero (the solitary wave) to infinity (the deep-water wave). The second parameter, the wave height or amplitude, varies from zero (the infinitesimal wave) to a limiting value dependent on the first parameter. Solutions of limiting waves, with angled crests, have been presented in a previous paper; this paper considers near-limiting waves having rounded crests with a very small radius of curvature, in some cases as little as 0.0001 of the water depth.

† Present address: Admiralty Research Establishment, Portsdown, Cosham, Portsmouth, Hampshire PO6 4AA, U.K.

The computing method is a modification of the integral equation technique used for limiting waves. Two leading terms are again used to give a close approximation to the flow near the crest and hence minimize the number of subsequent terms needed; the form of these leading terms is suggested by earlier work of G. G. Stokes (*Mathematical and physical papers*, vol. 1, pp. 225–228. Cambridge University Press (1880)), M. A. Grant (*J. Fluid Mech.* **59**, 257–262 (1973)) and L. W. Schwartz (*J. Fluid Mech.* **62**, 553–578 (1974)). To achieve satisfactory accuracy, however, it is now necessary to add a set of dipoles above the crest in the complex potential plane, as previously used by M. S. Longuet-Higgins & M. J. H. Fox (*J. Fluid Mech.* **80**, 721–741 (1977)).

The results include the first fully detailed calculations of non-breaking waves having local surface slopes exceeding 30°. The local profile at the crest, despite its very small scale, is shown to tend with increasing wave height to the asymptotic self-similar form previously computed by Longuet-Higgins & Fox. Their predictions of an ultimate maximum slope of 30.37° and a vertical crest acceleration of $0.388g$ are supported.

The results agree well with earlier calculations for steep waves at the two extremes of solitary and deep-water waves. In particular, it is confirmed that in the approach to limiting height the phase velocity and certain integral quantities possess not only the well-known maximum but also a subsequent minimum, the first in the infinite series of extrema predicted theoretically by M. S. Longuet-Higgins & M. J. H. Fox (*J. Fluid Mech.* **85**, 769–786 (1978)).

Briefly considered also are the level of action of near-limiting deep-water waves, the decay of surface drift velocity from the limiting value and the method established for computing waves of all lesser heights.

1. Introduction

This paper continues the study of steep, irrotational, progressive, symmetrical gravity waves begun in Williams (1981), to be referred to as paper I. Paper I concerned waves of limiting height, whose crests are angled rather than rounded, as first shown by Stokes (1880). Theoretical expressions for the flow near the crest, due to Stokes (1880) and Grant (1973), were used to define two leading terms in an integral equation formulation, from which were obtained results of high accuracy yet of relatively compact form, with a maximum of eighty component terms. While several previous workers had explicitly included the first, Stokes, term in their solutions, none had used the second term suggested by Grant's work; it was shown in paper I that the inclusion of both terms was a prerequisite to the accuracy achieved. The solutions of paper I covered the full range of limiting waves, from the solitary wave, with infinite wavelength, to the deep-water wave, with infinite depth.

We are concerned in this paper, as in paper I, only with uniform or regular wave trains, in which all crests have the same form. We therefore exclude classes of irregular waves such as have been computed recently by Chen & Saffman (1980) and Olfe & Rottman (1980).

The work of paper I has been extended to waves of near-limiting height, having rounded crests with very sharp curvature. This proved to be a more difficult task than for limiting waves because Stokes's expression for the angled crest no longer applies, nor is there a known, simply expressible, alternative. Nevertheless, a suitable modification of the original algorithm has been found, and has yielded solutions for near-limiting waves whose accuracy is only a little short of those of paper I. The full range, from solitary to deep-water waves, has again been covered.

Two important features of near-limiting waves have been verified. Firstly, the local surface profile near the crest has been shown to tend with increasing height to the asymptotic self-similar form first computed in isolation by Longuet-Higgins & Fox (1977). Their profile predicted an

ultimate maximum slope of 30.37° and a vertical crest acceleration of 0.388g, both of which values are supported. Secondly, Longuet-Higgins & Fox (1978) have shown that in the approach to the limiting wave the phase velocity and several integral properties have not only the well-known maximum, first pointed out by Longuet-Higgins (1974, 1975), but also a subsequent infinite sequence of ever closer minima and maxima. The accuracy of the present results is sufficient to resolve the first of these minima.

Other previous computations of steep waves over a range of wavelengths include those of Sasaki & Murakami (1973), Schwartz (1974) and Cokelet (1977); in addition Longuet-Higgins & Fenton (1974) and Byatt-Smith & Longuet-Higgins (1976) have computed solitary waves, while Longuet-Higgins (1975) has solved deep-water waves. Only the work of Cokelet and Longuet-Higgins includes waves with surface slopes exceeding 30°, although they did not specifically compute the wave profiles.

Section 2 first summarizes the formulation of the problem, as presented in more detail in paper I, and §3 discusses previous analyses of near-limiting waves, especially that of Longuet-Higgins & Fox (1977, 1978). Section 4 then describes the modification of the original computing method for the near-limiting wave and §5 presents the results, as sets of defining coefficients and tabulated principal properties, and considers the accuracy.

Section 6 compares the crest profiles of the highest waves computed with the asymptotic form calculated in isolation by Longuet-Higgins & Fox. Sections 7 and 8 consider the two extremes of solitary and deep-water waves and compare the results with previous work. Section 9 presents detailed tabulations of selected near-limiting waves to complement the tables of paper I, and §10 considers briefly the decay of the strong surface drift velocity from the limiting values calculated in paper I. Finally, §11 describes in outline the method which has been successfully used for calculating waves of all lesser heights.

2. Formulation of the problem

The initial formulation is identical with that used for limiting waves in paper I, and will be recapitulated only briefly. With reference to figures 1, 2, 3, which are repeated from that paper, we consider as before progressive symmetrical, irrotational, inviscid waves propagated without change of form in liquid of uniform and finite depth. Figure 1 shows the flow, reduced to a steady state, in the physical plane of $z = x + \mathrm{i}y$, in which the wavelength is L, mean depth h and wave height H; figure 2 shows the plane of the complex potential $\chi = \phi + \mathrm{i}\psi$, defined such that surface and bed are given by $\psi = 0, -2$ respectively. In view of the periodic conditions, a further transformation is made to the τ-plane, figure 3, given by

$$\chi = \mathrm{i}(2/d)\ln\tau, \quad \tau = \rho\,\mathrm{e}^{\mathrm{i}\theta}, \tag{2.1}$$

where

$$d = 4\pi/\lambda, \tag{2.2}$$

with λ being the period in the χ-plane of the velocity potential ϕ. The inner circle in the τ-plane, $\rho = R = \exp(-d)$, represents the bed, while the outer unit circle represents the surface.

Figure 1 shows waves of both infinitesimal and finite amplitude; whereas they are defined to have common domains in the χ- and τ-planes, their wavelengths, mean depths and total energy levels generally differ in the physical plane. The variable F^2 is defined such that acceleration due to gravity g is equal to $1/2F^2$, F being also the Froude number of the infinitesimal wave. The factor α accounts for the movement of the total energy line between the infinitesimal and finite-amplitude conditions.

Field variables include the horizontal and vertical velocities u, v of the steady motion and the ratio of pressure to density p, which is related to the velocities by Bernoulli's equation,

$$p+\tfrac{1}{2}(u^2+v^2)-\tfrac{1}{2}y/F^2-\tfrac{1}{2}(\alpha-1)=0. \tag{2.3}$$

Each required solution is a harmonic function, $z(\chi)$ or $z(\tau)$, symmetrical at the crest and trough planes, having the bed as a solid boundary and satisfying the Bernoulli condition (2.3) at the surface, where $p=p_s\equiv 0$. In the χ-plane this may be written

$$\frac{1}{2}\left[\frac{\mathrm{Im}\,(z)}{F^2}+\alpha-1-\frac{1}{|\,\mathrm{d}z/\mathrm{d}\chi\,|^2}\right]=p_s\equiv 0,\ \psi=0, \tag{2.4}$$

while in the τ-plane it is

$$\frac{1}{2}\left[\frac{\mathrm{Im}\,(z)}{F^2}+\alpha-1-\frac{1}{|\,\tfrac{1}{2}d\tau\,\mathrm{d}z/\mathrm{d}\tau\,|^2}\right]=p_s\equiv 0,\ \rho=1. \tag{2.5}$$

Solutions are sought for the full range $\infty\geqslant\lambda\geqslant 0$ or $0\leqslant d\leqslant\infty$, corresponding in the τ-plane to $1\geqslant R\geqslant 0$. The extremes, however, cannot be computed specifically and it is shown in paper I that a practical computing range for steep waves is $0.2\leqslant d\leqslant 10.0$. To working accuracy, the extremes of solitary and deep-water waves may then be deduced from solutions for $d=0.2$, 10.0 respectively.

We shall continue with the technique of paper I, whereby the full solution in the τ-plane comprises a linear combination of partial solutions, each being a symmetrical harmonic function satisfying identically the bed condition

$$\mathrm{Re}\,(\tau\,\mathrm{d}z/\mathrm{d}\tau)=0,\quad \rho=R, \tag{2.6}$$

but not in general the nonlinear free-surface condition (2.5). The coefficients are determined iteratively such that the combination satisfies (2.5) at a discrete set of nodal points stationed, in view of symmetry, on the upper semicircle, $\rho=1$, $0\leqslant\theta\leqslant\pi$.

The solutions of paper I are in the form

$$z=z_0+\zeta,\quad \zeta=\xi+\mathrm{i}\eta, \tag{2.7}$$

where

$$z_0=-\mathrm{i}(2/d)\,\ln\tau+\mathrm{i}F^2, \tag{2.8}$$

and ζ is a linear combination of partial solutions in the following forms:

$$\zeta_0=-\mathrm{i}(1/d)\,\ln\,(\tau/R), \tag{2.9}$$

$$\zeta_m=-\frac{\mathrm{i}}{1-R^{2m}}\left[\tau^m-\left(\frac{R^2}{\tau}\right)^m\right],\quad m=1,2,\ldots,\infty, \tag{2.10}$$

$$\zeta_{m,A,\nu}=\frac{\mathrm{i}\{[A^{-1}-\tau^m]^\nu-[A^{-1}-(R^2/\tau)^m]^\nu\}}{[A^{-1}-R^{2m}]^\nu-[A^{-1}-1]^\nu}. \tag{2.11}$$

Each of these partial solutions that contribute to ζ is normalized to take the value $-\mathrm{i}$ at the crest, $\tau=1$. We note that the last form $\zeta_{m,A,\nu}$ degenerates to ζ_m when A tends to zero.

The quantity $p_s(\theta)$ in (2.5) is a surface pressure distribution which should ideally be identically zero at the end of the computation but in practice will be zero only at the nodal points. It is convenient to regard the computed solutions as exact, with an accepted distribution

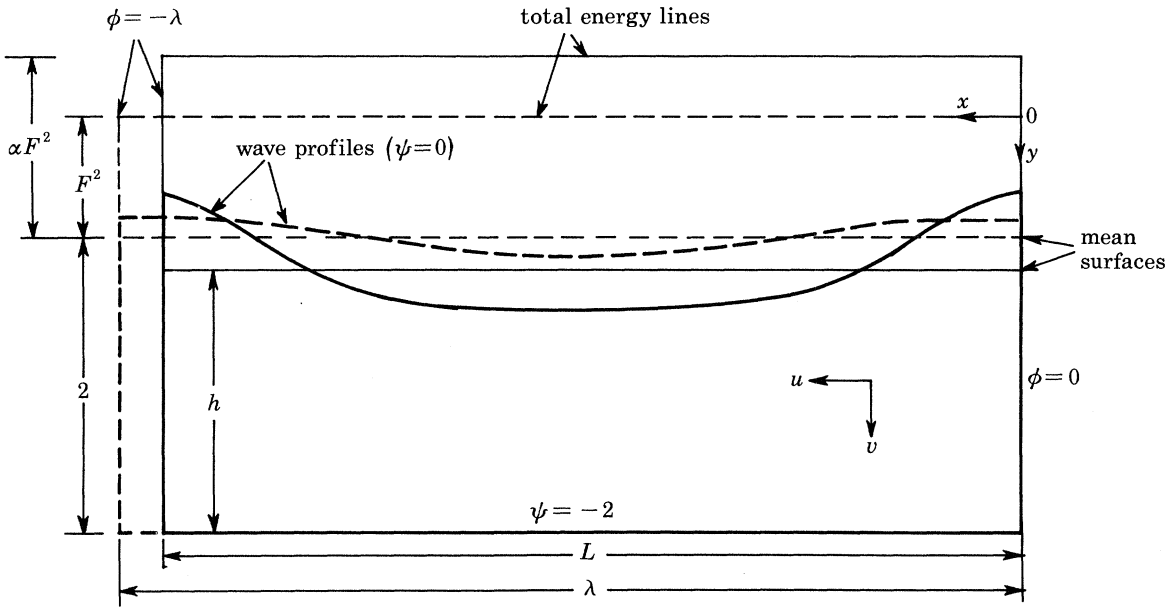

FIGURE 1. The z-plane; ---, ––– infinitesimal wave; ——, —— finite wave.

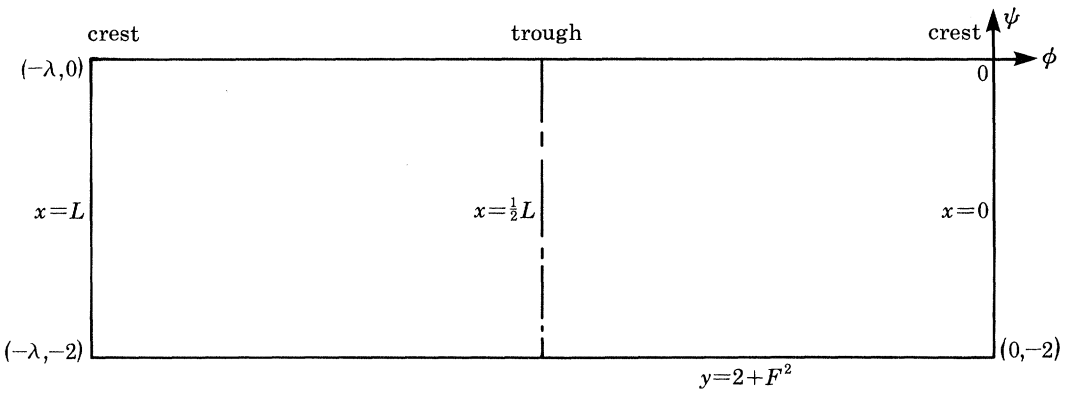

FIGURE 2. The χ-plane.

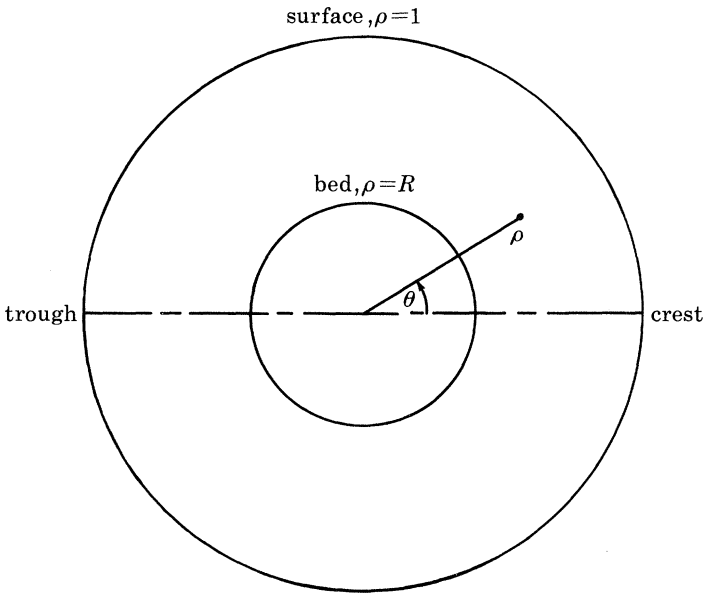

FIGURE 3. The τ-plane.

PHILOSOPHICAL TRANSACTIONS OF THE ROYAL SOCIETY A MATHEMATICAL, PHYSICAL & ENGINEERING SCIENCES

$p_s(\theta)$, and to compare them with the ideal solution, $p_s \equiv 0$, by means of error quantities derived from p_s. These error quantities include the maximum modulus over a wavelength, $\hat{p}_s$, the equivalent relative surface elevation error $\epsilon(\theta)$, given by

$$\epsilon(\theta) = 2F^2 p_s(\theta)/H, \tag{2.12}$$

and the root mean square of $\epsilon(\theta)$, denoted by ϵ^*. Paper I ((4.11)–(4.13)) defines also three quantities P_1, P_2, P_3, comprising integrals over the wavelength of expressions involving $p_s(\theta)$. These integrals were introduced in the reworking of Longuet-Higgins's (1974, 1975) integral relationships for non-zero p_s.

3. Previous analysis of near-limiting waves

Paper I discusses conditions at the angled crest of a limiting wave, considered first by Stokes (1880) and later by Grant (1973). With Z defined to move the space origin temporarily to the crest, the flow near $\chi = 0$ is of the form

$$\mathrm{i}Z = -(3F/\sqrt{2})^{\frac{2}{3}}(\mathrm{i}\chi)^{\frac{2}{3}} + C(\mathrm{i}\chi)^{\mu} + \ldots, \tag{3.1}$$

where C is a real coefficient.

The first term represents the 120° crest angle of the Stokes corner flow; the second term arises from Grant's analysis. The exponent μ is given by

$$\mu = -2K/\pi - \tfrac{1}{3}, \tag{3.2}$$

where K is a negative real root of the transcendental equation

$$K \tan K = -\tfrac{1}{2\sqrt{3}}\pi. \tag{3.3}$$

The first, and dominating, root is $K = -2.832$, giving $\mu = 1.469$.

For near-limiting waves, Longuet-Higgins & Fox (1977) examine the form of the free surface in the zone near the crest whose size is of order l, the small distance of the crest below the total energy line. They argue that in the limit the motion depends only on the dimension l, acceleration due to gravity g (represented in our notation by $1/2F^2$) and the asymptotic form of the surface, which at distances large compared with l must tend to the profile of the Stokes corner flow, represented by the first term of (3.1). This leads them to expect a family of self-similar flows, which they compute by two independent methods, a numerical treatment using dipoles and a full analytical method. Comparisons of this asymptotic inner profile with the inner crest profiles of the present solutions will be made in §6.

Longuet-Higgins & Fox show further that at great distance the asymptotic approach of their inner profile to the Stokes corner profile with slope 30° is not monotonic but oscillatory, the initial approach to the asymptote being from above and accounting for surface slopes locally exceeding 30°. The oscillation decays according to $r^{-\frac{1}{2}}$, r being the distance from the crest, and is governed by the imaginary roots, $K = \pm 1.122\mathrm{i}$, of the same transcendental equation (3.3). The relevant exponents, again given by (3.2), are $-\frac{1}{3} \pm 0.714\mathrm{i}$. (Longuet-Higgins & Fox use K to denote what would be $-\mathrm{i}K$ in the present notation, their corresponding equation being $K \tanh K = \frac{1}{2\sqrt{3}}\pi$.)

In a second paper Longuet-Higgins & Fox (1978) consider an intermediate zone of the flow

in a near-limiting wave, whose scale is large in relation to the inner profile but small compared with the wave as a whole. Within this zone can be expected features of both the asymptotic behaviour of the inner profile at infinity and the form of the limiting wave near the crest. Thus, they postulate for this region an expansion of the form

$$iZ = -(3F/\sqrt{2})^{\frac{2}{3}}(i\chi)^{\frac{2}{3}} + C(i\chi)^{1.469} + D(i\chi)^{-\frac{1}{3}+0.714i} + D^*(i\chi)^{-\frac{1}{3}-0.714i} + \ldots, \tag{3.4}$$

where D is complex and D^* is its conjugate. Regarding this expansion as an expression of the small departure of a near-limiting wave from limiting form, they then use it to derive the phase velocity and several integral properties of near-limiting waves. Their results are presented as expansions of the small parameter ϵ' (denoted ϵ by Longuet-Higgins & Fox) given by

$$\epsilon' = u_{sc}/2^{\frac{1}{2}}c_0, \tag{3.5}$$

where u_{sc} is, for the steady motion of figure 1, the value of the horizontal velocity u on the surface at the crest. The reference quantity c_0 is the phase velocity of the infinitesimal wave having the same depth h and wavelength L, given (Lamb 1932) by

$$c_0 = \left(\frac{L}{4\pi F^2}\tanh\frac{2\pi h}{L}\right)^{\frac{1}{2}}. \tag{3.6}$$

Longuet-Higgins & Fox, pursuing their analysis for deep-water waves only, derive expansions in ϵ' correct to order ϵ'^3; they show that, although their working expansion (3.4) does not accurately represent the inner profile, the contributions to the integrals from the inner zone are of a higher order than ϵ'^3. These expansions will be considered further in the discussion of deep-water waves in §8.

The present objective is to compute a complete definition of near-limiting waves, of sufficient accuracy to resolve the details of the inner zone. The inner profile must, therefore, be generated explicitly and the approach must be distinct from that of Longuet-Higgins & Fox. Clearly the first term at least of (3.4) must be adjusted, representing as it does a singularity at the wave crest; it is to be expected that for a near-limiting wave any singularity will be slightly above the crest. Grant (1973) discusses this, and shows that when the singularity leaves the crest its exponent can no longer be $\frac{2}{3}$ but can only be $\frac{1}{2}$. He concludes that in the passage to the limiting wave several singularities of order $\frac{1}{2}$ probably coalesce to give the limiting form of order $\frac{2}{3}$. This is corroborated by Longuet-Higgins & Fox (1978) who extend analytically their solution for the inner profile to the region above the free surface and demonstrate the presence of a singularity of order $\frac{1}{2}$.

Schwartz (1974), having computed steep waves by a high-order computer-aided series expansion, also considers the implied singularity above the crest and, like Grant, finds that its order is $\frac{1}{2}$ rather than $\frac{2}{3}$ for waves well below the highest. He demonstrates, however, that for waves close to the highest there is an apparent singularity of intermediate order, probably the effect of several neighbouring singularities of order $\frac{1}{2}$ in the process of coalescing in the limiting case.

From this previous work we deduce that, whereas the correct representation of a near-limiting wave should include several singularities of order $\frac{1}{2}$ positioned somewhere above the crest, we may be able to represent these adequately by a single singularity of higher order. This was the numerical approach first tried in the present work, as described in the next section.

PHILOSOPHICAL TRANSACTIONS OF THE ROYAL SOCIETY A MATHEMATICAL, PHYSICAL & ENGINEERING SCIENCES

4. Computing technique

Initial trials for near-limiting waves used the closest possible method to that established for limiting waves in paper I. The limiting-wave solutions use two leading terms of form $\zeta_{m,A,\nu}$, (2.11), namely $s\zeta_{1,1,\frac{2}{3}}$ and $q\zeta_{1,1,\mu}$, where s and q are coefficients and $\mu = 1.469$. The nodal points are placed at crest and trough, and uniformly between, with an additional node at a small angle θ_c (in the τ-plane) from the crest.

For near-limiting waves the singularity was moved away from the crest by reducing A slightly below unity in the leading terms, typically to 0.99 in the earliest runs. The exponent ν of the first term was also reduced below $\frac{2}{3}$, as indicated by the discussion of §3, the most suitable value being found by trial and error. Although the second exponent μ continues to appear in the expansion (3.4), it was realized that the empirical adjustment made to ν might call for a consequential change in μ. However, no clear improvement resulted from trial changes to μ, which was therefore left at its original value of 1.469.

With the reduction of A, and after trial-and-error variation of the leading exponent, reasonably accurate results were obtained for near-limiting waves, although this accuracy fell well short of that of paper I. The solutions at this stage showed large gradients of p_s in the small sharply curved inner profile zone and did not, therefore, give realistic representations of the local flow at the crest. This being so, the inclusion of the terms with complex exponent in (3.4) was not expected to help, since they accounted only for the outer extremes of the inner profile.

It was therefore decided, in an attempt to define the inner profile more precisely, to supplement the original two leading terms with a series of dipoles outside the flow area, distributed along the real axis in the τ-plane. This follows the initial method of Longuet-Higgins & Fox (1977) for computing the asymptotic inner profile in isolation. In the notation of (2.11) the dipoles are represented by $\zeta_{1,B,-1}$, with $B < A$.

Up to eight dipoles were eventually used, each being associated with a new nodal point in the inner profile zone. Despite the greatly differing scales of the inner profile and the overall wave, and the consequent non-uniform distribution of nodes, it was generally found that the algorithm continued to converge strongly, to yield the accurate solutions required.

Solutions have thus been computed in the following form:

$$z = z_0 + \zeta, \tag{4.1}$$

where

$$\zeta = s\zeta_{1,A,\nu} + q\zeta_{1,A,\mu} + \sum_{k=1}^{n} r_k \zeta_{1,B(k),-1} + \sum_{m=0}^{N-2} a_m \zeta_m. \tag{4.2}$$

The second exponent μ retains the value 1.469345741 used for limiting waves, while the positions of the dipoles and their associated nodes are given by

$$B(k) = 1 - 2j(1-A), \tag{4.3}$$

$$\theta_k = \tfrac{1}{2} j\pi(1-A), \tag{4.4}$$

with j taking selected values in the range 1–8.

A solution obtained in the form (4.2) may afterwards, if desired, be recast into an infinite series of basic terms

$$\zeta = \sum_{m=0}^{\infty} A_m \zeta_m, \tag{4.5}$$

using binomial expansions similar to those given for limiting waves in paper I ((6.1), (6.2)).

The iteration involves $N+n+2$ unknowns,

$$\alpha, s, q, r_1, r_2, \ldots, r_n, a_0, a_1, \ldots, a_{N-2},$$

and $N+n+2$ nodal points,

$$\theta = k\pi/N, \quad k = 0, 1, 2, \ldots, N; \quad \theta = \theta_c; \quad \theta = \theta_k, \quad k = 1, 2, \ldots, n.$$

The first seven columns of table 1 summarize the specifications of the cases computed; the remaining columns give the error quantities derived from $p_s(\theta)$, as defined in §2 and paper I.

TABLE 1. SPECIFICATION OF CASES COMPUTED (DEFINED IN (4.1)–(4.4)) AND ERROR QUANTITIES

d	N	A	ν	θ_c	n	$j_k, k = 1, 2, \ldots, n$	$10^6\hat{p}_s$	$10^6\,\epsilon^*$	$10^6 P_1$	$10^6 P_2$	$10^6 P_3$
0.2	79	†0.99999	0.6615	$\pi/4000$	6	1, 2, 3, 4, 6, 8	34	1	0.0	0.0	0.0
		0.99995	0.652	$\pi/1200$	6	1, 2, 3, 4, 6, 8	46	5	−0.5	−0.6	−0.1
		0.9999	0.647	$\pi/800$	6	1, 2, 3, 4, 6, 8	22	2	0.0	0.0	0.0
		0.999	0.580	$\pi/280$	4	1, 2, 3, 4	17	2	−0.1	−0.1	0.0
		0.998	0.571	—	4	1, 2, 3, 4	41	4	−0.1	−0.2	0.0
		0.997	0.578	—	4	1, 2, 3, 4	17	2	0.1	0.1	0.0
		0.996	0.572	—	4	1, 2, 3, 4	16	1	0.0	0.0	0.0
		0.995	0.566	—	4	1, 2, 3, 4	18	0	0.0	0.0	0.0
		0.994	0.560	—	4	1, 2, 3, 4	19	0	0.0	0.0	0.0
		0.99	0.520	—	2	1, 2	8	0	−0.1	−0.1	0.0
0.5	41	0.99999	0.6635	$\pi/4000$	6	1, 2, 3, 4, 6, 8	41	1	0.4	0.4	0.0
		0.9999	0.652	$\pi/800$	6	1, 2, 3, 4, 6, 8	31	3	−0.1	−0.1	0.0
		0.999	0.612	$\pi/280$	4	1, 2, 3, 4	15	1	0.3	0.3	0.1
		0.99	0.525	—	1	1	6	1	0.0	0.0	0.0
1.0	26	†0.99999	0.664	$\pi/4000$	6	1, 2, 3, 4, 6, 8	33	2	−0.1	0.0	−0.1
		†‡0.9999	0.655	$\pi/800$	6	1, 2, 3, 4, 6, 8	37	5	−0.5	−0.3	−0.1
		0.999	0.618	$\pi/280$	4	1, 2, 3, 4	21	4	−0.2	−0.1	0.0
		0.99	0.523	$\pi/280$	2	1, 2	7	1	0.3	0.2	0.1
2.0	20	0.99999	0.6645	$\pi/4000$	8	1, 2, …, 8	31	2	−0.2	−0.1	0.0
		0.99999	0.6645	$\pi/4000$	7	1, 2, …, 7	35	2	0.4	0.2	0.0
		0.9999	0.657	$\pi/800$	8	1, 2, …, 8	35	6	−0.8	−0.3	−0.1
		0.999	0.631	$\pi/280$	6	1, 2, 3, 4, 6, 8	14	2	−0.5	−0.2	0.0
		0.99	0.523	$\pi/280$	4	1, 2, 3, 4	5	1	0.0	0.0	0.0
10.0	19	†0.99999	0.6645	$\pi/4000$	8	1, 2, …, 8	29	3	−0.5	0.0	0.0
		0.99999	0.6645	$\pi/4000$	7	1, 2, …, 7	34	2	0.1	0.0	0.0
		†§0.9999	0.657	$\pi/800$	8	1, 2, …, 8	42	7	−1.3	−0.1	0.0
		0.9998	0.653	$\pi/800$	8	1, 2, …, 8	45	5	0.8	0.1	0.0
		0.999	0.631	$\pi/280$	6	1, 2, 3, 4, 6, 8	19	3	−0.8	−0.1	0.0
		0.996	0.603	$\pi/280$	6	1, 2, 3, 4, 6, 8	10	2	0.2	0.0	0.0
		0.994	0.541	$\pi/66$	6	1, 2, 3, 4, 6, 8	11	2	−0.2	0.0	0.0
		0.992	0.529	$\pi/280$	6	1, 2, 3, 4, 6, 8	15	3	−0.3	0.0	0.0
		0.99	0.523	$\pi/280$	4	1, 2, 3, 4	6	1	0.1	0.0	0.0

† Included in table 2. ‡ Detailed in table 8. § Detailed in table 9.

The new set of nodal points is disposed in the physical plane within a lateral distance of about $10l$ from the crest. Although, as will be shown in §6, the maximum slope of the surface profile generally occurs beyond this zone, convergence failed if an attempt was made to extend the nodes further. It was found also that the distribution of the crest nodes could not depart significantly from uniform spacing without destroying convergence. The schemes shown in table 1 therefore define the apparent limits of the method. It will be shown, however, that most details of the wave motion are very well defined; only the precision of the maximum surface slope remains slightly unsatisfactory by the high standards of accuracy generally achieved.

The new nodal points are generally closer to the crest than the original auxiliary crest node θ_c, introduced for limiting wave solutions. For the highest values of A it was found advantageous to reduce θ_c itself to as little as $\frac{1}{4000}\pi$, but for lower values the original value of $\frac{1}{280}\pi$ was retained, although in some cases this fell within the range of the new nodes. The choice of nodes was much less critical for values of A less than about 0.999, provided only that interference was guarded against; for example, table 1 ($d = 10.0$, $A = 0.994$) shows one case in which θ_c was changed for this reason. In seven cases, θ_c was eliminated entirely, q then being set to zero in (4.2).

For $d = 1.0$, 2.0, 10.0 the iteration was conducted as for limiting waves, being terminated when successive steps changed no coefficient by more than a small tolerance, generally 10^{-8}. For $d = 0.2$, 0.5 this technique gave an oscillating behaviour, indicating presumably that two alternative sets of coefficients were capable of describing the wanted solution. In these cases, therefore, the iteration was terminated when the maximum nodal error was of modulus less than 10^{-7}, which condition was reached before the oscillating behaviour appeared. These solutions are, of course, entirely satisfactory for defining the wave motion, their only disadvantage being that a series of computed sets of coefficients will not constitute a family that could be used for interpolation.

5. Results and discussion of accuracy

The numerical results are necessarily presented only briefly in this paper; more extensive tables are to be found in the author's Ph.D. thesis (Williams 1983).

Table 2 shows the computed coefficients for five of the thirty-two cases listed in table 1; the cases chosen all have local surface slopes exceeding 30°, as will be shown subsequently.

Whereas the parameter A is central to the numerical formulation, it is more relevant in discussing the solutions to consider the quantity ω defined by Longuet-Higgins (1975). Let u_{sc}, u_{st} denote the velocities on the surface at the crest and trough respectively in the steady flow (figure 1) and let

$$c = \lambda/L \tag{5.1}$$

be the celerity, or phase velocity, needed to bring the space-mean velocity at the bed to zero over a wavelength. Then

$$\omega = 1-(u_{sc}\,u_{st}/cc_0)^2 = 1-2(\epsilon' u_{st}/c)^2, \tag{5.2}$$

where c_0 is defined by (3.6) and ϵ' by (3.5).

The value of ω, which varies from zero for infinitesimal waves to unity for limiting waves, is included in the results illustrated in table 2.

Table 3 gives selected properties of the waves for twenty of the solutions of table 1, headed

Table 2. Computed coefficients for selected solutions

d	0.2		1.0	1.0	10.0	10.0
A	0.99999		0.99999	0.9999	0.99999	0.9999
ω	0.99826		0.99916	0.99612	0.99924	0.99648
	† $\times 10^8$		$\times 10^8$	$\times 10^8$	$\times 10^9$	$\times 10^9$
α	109326767		108562209	108560378	103085638	103144018
s	353312894		214190667	204260132	259298237	249292559
q	93373191		60714437	50756488	69977303	60780107
r_1	21404		6844	29499	7726	33003
r_2	35752		12075	41009	13046	48272
r_3	−24612		−9495	−12095	−17142	−36437
r_4	73834		26887	57094	101443	220042
r_5	−65692		−25070	−33587	−294615	−550344
r_6	79508		29300	55660	558527	998104
r_7					−559578	−972843
r_8					237037	422197
a_0	−24942266		−13314297	−13313942	−114283210	−114274560
a_1	−377917390		−195882996	−172268631	−220113421	−198367075
	57563602		15091021	11776686	13849032	11438892
	5428032		1340418	904329	1136659	845366
	870865		296722	167728	236165	155801
$a_{5,40}$	117352	−202	93480	42070	69931	40136
	−16788	−181	35756	11726	25043	12184
	−31974	−162	15454	3064	10060	4002
	−26183	−144	7254	436	4343	1339
	−19110	−129	3608	−314	1958	428
$a_{10,45}$	−13911	−115	1870	−456	902	118
	−10439	−103	998	−410	417	19
	−8133	−92	543	−319	189	−7
	−6552	−82	299	−232	82	−9
	−5420	−73	165	−161	33	−6
$a_{15,50}$	−4570	−65	91	−107	12	−3
	−3905	−58	50	−69	3	−1
	−3368	−52	27	−43		
	−2923	−46	14	−25		
	−2548	−41	7	−14		
$a_{20,55}$	−2229	−36	3	−7		
	−1954	−32	1	−3		
	−1717	−28	1	−1		
	−1511	−25				
	−1332	−22				
$a_{25,60}$	−1176	−19				
	−1039	−17				
	−919	−14				
	−814	−12				
	−722	−11				
$a_{30,65}$	−641	−9				
	−569	−8				
	−506	−6				
	−450	−5				
	−401	−4				
$a_{35,70}$	−357	−3				
	−319	−3				
	−284	−2				
	−254	−1				
	−227	−1				
a_{75}		−1				

† Results quoted have been multiplied by the given factor, i.e. in the first column $\alpha = 109326767 \times 10^{-8}$, etc.

PHILOSOPHICAL TRANSACTIONS OF THE ROYAL SOCIETY A MATHEMATICAL, PHYSICAL & ENGINEERING SCIENCES

Table 3. Properties of selected waves

(For each d, A takes the values 0.99999, 0.9999, 0.999, 0.99.)

		$d = 0.20$, $1/2F^2 = 0.506649$, $H_{\max} = 1.39940$, $\sigma_t^2 = 0.000000$			
relative height parameter	ω	0.99826	0.99202	0.96449	0.84292
total head relative to crest	l	0.001406	0.006447	0.028684	0.126854
mean depth	h	1.78063	1.78057	1.77957	1.78375
wavelength	L	54.996	54.994	54.955	55.075
wave height	H	1.3979	1.3929	1.3729	1.2724
total head relative to bed	$2+\alpha F^2$	3.07892	3.07894	3.07983	3.07890
mean depth/wavelength	h/L	0.032377	0.032377	0.032382	0.032388
height/mean depth	H/h	0.7851	0.7823	0.7715	0.7134
celerity (zero mean velocity)	c	1.14248	1.14251	1.14332	1.14084
celerity (zero mass transport)	c'	1.12320	1.12323	1.12387	1.12123
depth parameter	$2h(Fc/L)^2$	0.001517	0.001517	0.001520	0.001511
height parameter	$2H(Fc/L)^2$	0.001191	0.001187	0.001173	0.001078
mean momentum	I	0.03433	0.03433	0.03462	0.03498
mean kinetic energy	T	0.01961	0.01961	0.01979	0.01995
mean potential energy	V	0.01651	0.01651	0.01665	0.01693
radiation stress	S_{xx}	0.04724	0.04724	0.04764	0.04836
mean energy flux	E	0.04014	0.04014	0.04052	0.04088
bed velocity variance	σ_b^2	0.01030	0.01029	0.01036	0.01085
		$d = 0.50$, $1/2F^2 = 0.540988$, $H_{\max} = 1.36616$, $\sigma_t^2 = 0.000000$			
relative height parameter	ω	0.99894	0.99514	0.97802	0.90281
total head relative to crest	l	0.000748	0.003437	0.015542	0.068556
mean depth	h	1.87626	1.87625	1.87585	1.87703
wavelength	L	22.8322	22.8322	22.8251	22.8258
wave height	H	1.3654	1.3627	1.3514	1.3023
total head relative to bed	$2+\alpha F^2$	3.01235	3.01234	3.01266	3.01425
mean depth/wavelength	h/L	0.082176	0.082176	0.082184	0.082233
height/mean depth	H/h	0.72771	0.72627	0.72040	0.69383
celerity (zero mean velocity)	c	1.10076	1.10076	1.10110	1.10107
celerity (zero mass transport)	c'	1.06595	1.06596	1.06619	1.06551
depth parameter	$2h(Fc/L)^2$	0.008061	0.008061	0.008069	0.008073
height parameter	$2H(Fc/L)^2$	0.005866	0.005854	0.005813	0.005602
mean momentum	I	0.06531	0.06530	0.06550	0.06673
mean kinetic energy	T	0.03594	0.03594	0.03606	0.03674
mean potential energy	V	0.03132	0.03132	0.03141	0.03210
radiation stress	S_{xx}	0.08275	0.08274	0.08299	0.08463
mean energy flux	E	0.06844	0.06843	0.06868	0.06998
bed velocity variance	σ_b^2	0.01756	0.01755	0.01758	0.01811
		$d = 1.0$, $1/2F^2 = 0.656518$, $H_{\max} = 1.20900$, $\sigma_t^2 = 0.00012$			
relative height parameter	ω	0.99916	0.99612	0.98244	0.92239
total head relative to crest	l	0.000442	0.002034	0.009218	0.040639
mean depth	h	1.94111	1.94111	1.94087	1.94173
wavelength	L	11.7298	11.7298	11.7277	11.7262
wave height	H	1.2085	1.2069	1.2001	1.1721
total head relative to bed	$2+\alpha F^2$	2.82680	2.82679	2.82688	2.82818
mean depth/wavelength	h/L	0.165485	0.165484	0.165495	0.165589
height/mean depth	H/h	0.62260	0.62176	0.61831	0.60366
celerity (zero mean velocity)	c	1.07132	1.07132	1.07151	1.07165
celerity (zero mass transport)	c'	1.03034	1.03034	1.03046	1.03001
depth parameter	$2h(Fc/L)^2$	0.024664	0.024664	0.024678	0.024702
height parameter	$2H(Fc/L)^2$	0.015356	0.015335	0.015259	0.014912
mean momentum	I	0.07955	0.07954	0.07967	0.08085
mean kinetic energy	T	0.04261	0.04261	0.04268	0.04332
mean potential energy	V	0.03822	0.03822	0.03827	0.03891
radiation stress	S_{xx}	0.08532	0.08531	0.08545	0.08669
mean energy flux	E	0.07148	0.07147	0.07162	0.07265
bed velocity variance	σ_b^2	0.01522	0.01522	0.01522	0.01551

PHILOSOPHICAL TRANSACTIONS OF THE ROYAL SOCIETY A MATHEMATICAL, PHYSICAL & ENGINEERING SCIENCES

TABLE 3 (*continued*)

		$d = 2.0$, $1/2F^2 = 1.037315$, $H_{max} = 0.79997$			
relative height parameter	ω	0.99923	0.99644	0.98376	0.92892
total head relative to crest	l	0.000239	0.001102	0.005027	0.021951
mean depth	h	1.94083	1.94083	1.94062	1.94105
wavelength	L	5.9191	5.9191	5.9183	5.9174
wave height	H	0.79972	0.79883	0.79508	0.78028
total head relative to bed	$2+\alpha F^2$	2.48553	2.48553	2.48548	2.48610
mean depth/wavelength	h/L	0.327892	0.327890	0.327902	0.328024
height/mean depth	H/h	0.41205	0.41159	0.40970	0.40199
celerity (zero mean velocity)	c	1.06151	1.06151	1.06166	1.06182
celerity (zero mass transport)	c'	1.03049	1.03049	1.03060	1.03037
depth parameter	$2h(Fc/L)^2$	0.060174	0.060173	0.060201	0.060251
height parameter	$2H(Fc/L)^2$	0.024795	0.024767	0.024665	0.024220
mean momentum	I	0.06020	0.06020	0.06027	0.06104
mean kinetic energy	T	0.03195	0.03195	0.03199	0.03241
mean potential energy	V	0.02885	0.02885	0.02888	0.02928
radiation stress	S_{xx}	0.04759	0.04758	0.04767	0.04821
mean energy flux	E	0.04396	0.04395	0.04404	0.04456
bed velocity variance	σ_b^2	0.00327	0.00326	0.00327	0.00332
trough velocity variance	σ_t^2	0.00184	0.00184	0.00184	0.00186
		$d = 10.0$, $1/2F^2 = 5.000000$, $H_{max} = 0.167135$, $\sigma_b^2 = 0.00000$			
relative height parameter	ω	0.99924	0.99648	0.98396	0.92976
total head relative to crest	l	0.0000484	0.0002231	0.0010178	0.0044465
mean depth	h	1.89782	1.89783	1.89758	1.89743
wavelength	L	1.18483	1.18484	1.18467	1.18449
wave height	H	0.16708	0.16691	0.16614	0.16315
total head relative to bed	$2+\alpha F^2$	2.01031	2.01031	2.01010	2.00999
mean depth/wavelength	h/L	1.601765	1.601764	1.601776	1.601903
height/mean depth	H/h	0.08804	0.08795	0.08756	0.08599
celerity (zero mean velocity)	c	1.06061	1.06060	1.06075	1.06091
celerity (zero mass transport)	c'	1.05384	1.05384	1.05397	1.05406
depth parameter	$2h(Fc/L)^2$	0.30414	0.30414	0.30427	0.30444
height parameter	$2H(Fc/L)^2$	0.02678	0.02675	0.02664	0.02618
mean momentum	I	0.012837	0.012835	0.012851	0.013011
mean kinetic energy	T	0.006808	0.006807	0.006816	0.006902
mean potential energy	V	0.006146	0.006145	0.006151	0.006234
radiation stress	S_{xx}	0.008792	0.008790	0.008808	0.008904
mean energy flux	E	0.008624	0.008623	0.008639	0.008738
trough velocity variance	σ_t^2	0.00227	0.00227	0.00227	0.00230

in each case by the value of ω. Properties mentioned, in addition to those already defined, include:

the height H_{max} of the corresponding limiting wave (taken from paper I);

an alternative celerity $c' = 2/h$, bringing net mass transport at any vertical section to zero over a wave period;

the integral properties discussed by Longuet-Higgins (1975) and defined fully in paper I. They include the mean densities over a wavelength of momentum I (paper I, (4.5)), kinetic energy T (I, (4.6)) and potential energy V (I, (4.7)); the radiation stress S_{xx} (I, (4.8)) and mean energy flux E (I, (4.9));

the variances σ_b^2, σ_t^2 of the velocity distribution along the bed and beneath the trough, defined by (4.14), (4.15) of paper I.

The solutions, as shown by table 2, give compact representations of near-limiting waves, which have not been achieved before, but are less elegant than the limiting-wave solutions of

paper I. The main sequences of coefficients decay less rapidly to zero and in some cases change sign. The coefficients of the dipole terms vary erratically in magnitude and sign, although it should be noted that Longuet-Higgins & Fox (1977) obtained similar behaviour in their original calculation of the inner profile. For solutions involving six to eight dipoles there is a tendency for successive coefficients to become equal and opposite; in fact attempts to use more dipoles usually failed because such pairs of coefficients increased in magnitude without apparent limit at successive iterations.

The error quantities shown in table 1 are generally larger than for the corresponding limiting-wave solutions (paper I, table 2), but nevertheless show that a high accuracy has been achieved. The maximum surface pressure $\hat{p}_s$ in no case exceeds 5×10^{-5}, ϵ^* does not exceed 7×10^{-6} and the greatest of the pressure integrals P_1, P_2, P_3 has modulus 1.3×10^{-6}.

6. The inner profile near the crest

The asymptotic inner profile calculated by Longuet-Higgins & Fox (1977) and discussed in §3 has a maximum slope of 30.37° and a vertical crest acceleration of $0.388g$. The principal features of the inner profiles of the present solutions are given for comparison in table 4, which includes some further error quantities based on the surface pressure distribution $p_s(\theta)$. As the scale of the inner profile diminishes it will theoretically approach the asymptotic form but on the other hand will become progressively less well resolved in the computed solution. As a measure of this resolution, the local maximum modulus of p_s over a particular range is multiplied by $2F^2$ to convert it to a displacement error and divided by the profile scale l, to define a quantity $\hat{\delta}$. Three values, $\hat{\delta}_1$, $\hat{\delta}_2$, $\hat{\delta}_3$, have been calculated for each inner profile, applicable to the ranges $0 \leqslant x/l \leqslant 3$, $3 < x/l \leqslant 7.5$, $7.5 < x/l \leqslant 25$ respectively, and are shown in table 4.

Table 4. Properties of inner profiles, with error quantities

d	A	l	computed max. slope/deg	max. slope position, x/l	crest acceleration/g	$10^6\hat{\delta}_1$	$10^6\hat{\delta}_2$	$10^6\hat{\delta}_3$
0.2	0.99999	0.001406	30.35	14.9	0.3890	776	81	41200
	0.9999	0.006447	29.98	12.8	0.3876	641	30	3310
	0.999	0.028684	28.56	9.3	0.3811	433	47	1200
	0.99	0.126854	23.47	5.9	0.3430	132	16	22
0.5	0.99999	0.000748	30.40	15.2	0.3891	805	114	50100
	0.9999	0.003437	30.17	14.0	0.3884	656	34	5220
	0.999	0.015542	29.35	10.6	0.3852	589	53	1750
	0.99	0.068556	26.27	7.1	0.3666	155	126	121
1.0	0.99999	0.000442	30.41	15.3	0.3892	820	131	52100
	0.9999	0.002034	30.26	14.6	0.3886	663	35	6670
	0.999	0.009218	29.73	11.9	0.3867	609	55	2230
	0.99	0.040639	27.65	8.2	0.3756	10	267	269
2.0	†0.99999	0.000239	30.40	16.2	0.3890	710	48	37500
	‡0.99999	0.000238	30.42	15.3	0.3888	445	178	54500
	0.9999	0.001102	30.29	15.3	0.3887	667	32	3270
	0.999	0.005027	29.92	12.6	0.3874	610	32	1000
	0.99	0.021951	28.37	8.9	0.3797	45	26	237
10.0	†0.99999	0.0000484	30.40	16.2	0.3890	711	50	37400
	‡0.99999	0.0000482	30.42	15.5	0.3888	448	178	54400
	0.9999	0.0002231	30.30	15.3	0.3888	667	32	3230
	0.999	0.0010178	29.95	13.0	0.3876	610	32	1370
	0.99	0.0044465	28.49	9.2	0.3804	45	26	263

† Eight dipoles. ‡ Seven dipoles.

The low values of $\hat{\delta}_2$ in table 4 show that the inner profile is generally best resolved over the second range. The table also shows that resolution depends primarily on the size of the profile in the τ-plane, indicated by $1-A$, rather than on its physical size l.

For $A = 0.99999$, the highest value computed, the crest acceleration lies within the range $0.3888g$ to $0.3892g$ for all values of d. Despite the considerable range of physical scale of these profiles, table 4 shows that they are of similar precision and may, therefore, be compared on an equal basis with the asymptotic profile of Longuet-Higgins & Fox; this comparison is made in table 5.

TABLE 5. COMPARISON OF INNER PROFILES FOR $A = 0.99999$ WITH THE ASYMPTOTIC PROFILE OF LONGUET-HIGGINS & FOX (1977)

($\Delta\tilde{x}/l$, $\Delta\tilde{y}/l$ are shown in roman type for positive p_s, italics for negative p_s and bold type at the position of maximum surface slope. Note $d = 2.0$ (with eight and seven dipoles) is not shown, being almost identical with $d = 10.0$.)

L.-H. & F.		this paper, $A = 0.99999$										L.-H. & F.
$-\phi F\sqrt{(2/l^3)}$	$\tilde{x}/l$	$10^4\,\Delta\tilde{x}/l$					$10^4\,\Delta\tilde{y}/l$					$\tilde{y}/l$
		$d = 0.2$	0.5	1.0	10.0 †	10.0 ‡	$d = 0.2$	0.5	1.0	10.0 †	10.0 ‡	
0	0.0000	0	*0*	0	*0*	0	0	*0*	0	*0*	0	1.0000
0.9938	0.6953	*−1*	*−1*	*−1*	*−1*	*−1*	*1*	*1*	*1*	*1*	*0*	1.0464
1.9895	1.3539	*−3*	*−3*	*−4*	*−3*	*−2*	*0*	*0*	*1*	*0*	*0*	1.1709
2.9892	1.9607	*−3*	*−4*	*−4*	*−3*	*−2*	*−3*	*−3*	*−2*	*−2*	*−1*	1.3448
3.9949	2.5182	*−2*	*−3*	*−4*	*−3*	−2	*−5*	*−4*	*−4*	*−3*	−1	1.5445
5.0086	3.0347	−1	−2	−2	−2	*−2*	−7	−5	−4	−4	*−1*	1.7564
6.0324	3.5187	1	−1	−2	−1	*−2*	−7	−5	−4	−4	*−1*	1.9732
7.0685	3.9772	3	0	0	0	*−1*	−7	−5	−4	−4	*−1*	2.1915
8.1193	4.4160	*3*	0	−1	0	*−2*	*−8*	−5	−4	−4	*−1*	2.4097
9.1873	4.8393	*5*	*1*	*0*	*0*	−2	*−8*	*−4*	*−3*	*−3*	0	2.6271
10.2749	5.2508	*6*	*1*	*0*	*1*	−2	*−9*	*−5*	*−3*	*−4*	0	2.8438
11.3849	5.6534	*7*	*1*	*−1*	*1*	−3	*−9*	*−4*	*−2*	*−3*	1	3.0598
12.5203	6.0495	*8*	2	−1	*1*	−3	*−10*	−4	−1	*−3*	1	3.2757
13.6844	6.4413	9	2	−1	1	*−3*	−10	−4	−1	−3	*2*	3.4919
14.8805	6.8307	10	2	−1	1	*−4*	−12	−4	−1	−3	*2*	3.7090
16.1126	7.2193	12	3	−1	2	*−4*	−12	−3	0	−2	*3*	3.9274
17.3848	7.6090	*12*	*2*	*−2*	*1*	*−5*	*−13*	*−4*	*0*	*−3*	3	4.1480
18.7017	8.0011	*13*	*2*	*−2*	*1*	*−5*	*−14*	*−3*	*1*	*−2*	4	4.3712
20.0684	8.3972	*15*	*3*	*−2*	*1*	*−6*	*−14*	*−3*	*2*	*−1*	5	4.5978
21.4908	8.7989	*17*	*3*	*−3*	1	*−6*	*−15*	*−3*	*2*	−1	*5*	4.8286
22.9753	9.2078	*18*	*3*	*−3*	1	*−7*	*−16*	*−2*	*3*	−1	*7*	5.0643
24.5291	9.6255	*20*	*3*	*−4*	1	*−8*	*−18*	*−2*	*3*	−1	*7*	5.3059
26.1606	10.0539	20	2	−5	*0*	−10	−19	−2	4	*0*	9	5.5542
27.8792	10.4947	22	2	−6	*0*	−11	−20	−1	5	*0*	10	5.8103
29.6958	10.9500	25	3	−6	1	*−12*	−21	−1	6	0	*11*	6.0754
31.6228	11.4223	26	2	−7	0	*−14*	−23	−1	7	0	*13*	6.3508
33.6748	11.9140	*29*	*2*	*−9*	*0*	*−15*	*−23*	*1*	*10*	*2*	*15*	6.6378
35.8690	12.4282	*30*	*0*	*−11*	*−1*	*−19*	*−24*	*2*	*12*	*2*	*18*	6.9383
38.2254	12.9681	*31*	*−2*	*−14*	*−2*	*−22*	*−25*	*4*	*15*	*3*	*21*	7.2541
40.7678	13.5376	*33*	*−4*	*−18*	*−2*	*−26*	*−27*	*5*	*17*	*3*	*23*	7.5876
43.5250	14.1414	*32*	*−9*	*−24*	*−4*	*−33*	*−29*	*6*	*20*	*5*	*26*	7.9412
46.5315	14.7847	**32**	*−14*	*−31*	*−6*	*−40*	**−31**	*8*	*22*	*7*	*29*	8.3181
49.8295	**15.4740**	*30*	**−21**	**−40**	*−9*	**−50**	*−36*	**7**	**23**	*8*	**30**	**8.7221**
53.4712	16.2170	*28*	*−30*	*−51*	**−13**	*−62*	*−43*	*4*	*22*	**8**	*30*	9.1577
57.5216	17.0232	*25*	*−40*	*−64*	*−18*	*−76*	*−51*	*0*	*20*	*10*	*29*	9.6302

† Eight dipoles. ‡ Seven dipoles.

The origin is taken temporarily on the total energy line above the crest with surface coordinates $\tilde{x}$, $\tilde{y}$ corresponding respectively to y, x as defined by Longuet-Higgins & Fox. The outer columns of table 5 give their computed profile, with $\tilde{x}/l$, $\tilde{y}/l$ tabulated as functions of $\phi F\sqrt{(2/l^3)}$. The remaining columns show the deviations $\Delta\tilde{x}/l$, $\Delta\tilde{y}/l$ of the present solutions from this profile. To indicate the fluctuations of the small surface-pressure error p_s, the entries are shown in roman type where p_s is positive and in italics where it is negative; the changes of sign usually occur at the nodal points. In addition, the entry nearest to the point of maximum slope of each profile is printed in bold type.

For $\tilde{x}/l < 7.5$ all profiles for $d \geqslant 0.5$ are very close to the asymptotic profile, the small discrepancies being consistent with the generally small values of $\hat{\delta}_2$ (table 4). The much larger values of $\hat{\delta}_1$ for the innermost zone evidently do not have a significant effect. For $d = 0.2$, however, the profile at $\tilde{x}/l = 7.5$ is distinctly above the asymptotic solution and since table 4 has shown that all solutions are of comparable quality this must be accepted as a genuine trend.

In most solutions for a given A not only are $\hat{\delta}$ values of comparable magnitude but also p_s exhibits a similar sequence of sign changes over the profile, raising the possibility of a common systematic error. In an attempt to break this pattern supplementary solutions have been computed for $d = 2.0$, 10.0, with seven dipoles instead of the original eight. This changes the sign of p_s over most of the profile, although not at the extreme crest nor in the outer zone, $\tilde{x}/l > 7.5$. The value of $\hat{\delta}_1$ is, however, almost halved (table 4), with an accompanying reduction of $0.0002g$ in the computed crest acceleration. The true acceleration is therefore expected to be about $0.3885g$ for these cases and is probably the same for the asymptotic solution, agreeing very closely with Longuet-Higgins & Fox's estimate of $0.388g$.

In the outer zone, $\tilde{x}/l > 7.5$, $\hat{\delta}_3$ is large, being less restrained by the additional nodes, which cannot extend throughout this region without destroying convergence. All solutions except for $d = 0.2$ now deviate below the asymptotic profile, giving computed maximum slopes exceeding Longuet-Higgins & Fox's value of 30.37°. Some estimate of the likely error in slope can be made from the seven-dipole solutions, which increase $\hat{\delta}_3$ by 50% and the slope by 0.02°. This would suggest a true maximum slope for these cases of about 30.36°, and in particular we may say that this applies to a deep-water wave (represented to sufficient accuracy by $d = 10.0$) with $\omega = 0.99924$. Longuet-Higgins & Fox (1977) show graphically that the maximum slope of both solitary and deep-water waves varies linearly with ω as ω nears unity. The slope of their line, together with the above values, indicates a maximum slope for $\omega = 1$ of about 30.38°, although the accuracy is not sufficient for the second decimal place to be stated firmly. Longuet-Higgins & Fox's calculation of the asymptotic profile in isolation remains the best estimate of maximum slope. I noted, however, in examining their table 3 (reproduced in the present table 5), that the maximum slope appeared to be almost 30.38°, rather than 30.37° as stated in their paper.

7. Solitary waves

It was shown in paper I that solutions for $d = 0.2$ define to working accuracy the corresponding steep solitary wave because the flow at the trough is sensibly uniform and may simply be extended indefinitely. The value of ω derived from this extrapolation is denoted by ω_∞. Table 6 summarizes the properties of near-limiting solitary waves deduced in this way; results for $\omega_\infty = 1$, the limiting wave, are taken from table 5 of paper I.

The symbols I, T, V now have a subscript ∞ to denote the alternative definitions for solitary

TABLE 6. PROPERTIES OF LIMITING AND NEAR-LIMITING SOLITARY WAVES

(Values are normalized such that acceleration due to gravity and undisturbed depth are each taken as unity. Values in parentheses are interpolated from Byatt-Smith & Longuet-Higgins (1976). Interpolated values giving maximum Froude number and maximum surface slope = 30.00° are shown in italics.)

ω_∞	H'	Froude no.	M_∞	C_∞	I_∞	T_∞	V_∞	max. surface slope/deg
1.00000	0.833197	1.290889	1.970319	1.714569	2.543463	0.535005	0.437670	30.00
0.99833	0.8323	1.29086	1.9702	1.7145	2.5432	0.5349	0.4376	30.3
0.99514	0.8307	1.29085	1.9699	1.7142	2.5429	0.5348	0.4375	30.15
0.9927								*30.00*
0.99232	0.8294	1.29089	1.9696	1.7139	2.5425	0.5348	0.4375	29.98
0.96582	0.8181	1.29242	1.9776	1.7194	2.5559	0.5405	0.4419	28.56
0.94595	0.8096	1.29355	1.9892	1.7290	2.5732	0.5460	0.4464	27.60
		(1.2934)		(1.730)		(0.546)	(0.447)	
0.92896	0.8018	1.29410	1.9997	1.7382	2.5878	0.5498	0.4497	26.82
		(1.2940)		(1.739)		(0.549)	(0.450)	
0.917		*1.29421*						
0.91440	0.7947	1.29421	2.0082	1.7461	2.5990	0.5520	0.4518	26.18
		(1.2941)		(1.746)		(0.552)	(0.452)	
0.90119	0.7878	1.29403	2.0152	1.7529	2.6077	0.5530	0.4531	25.61
		(1.2940)		(1.752)		(0.553)	(0.453)	
0.88887	0.7812	1.29361	2.0209	1.7589	2.6142	0.5533	0.4536	25.09
		(1.2936)		(1.756)		(0.552)	(0.453)	
0.84895	0.7576	1.29082	2.0332	1.7742	2.6244	0.5487	0.4515	23.47
		(1.2909)		(1.772)		(0.548)	(0.451)	

waves given, after Longuet-Higgins (1974), by (4.23)–(4.25) of paper I. Three new quantities are the excess mass M_∞ and circulation C_∞, defined by (I, (4.21), (4.22)), and H', the ratio of wave height to undisturbed depth. As in paper I, the values of table 6 are normalized according to Longuet-Higgins's definition, with acceleration due to gravity and the undisturbed depth at infinity each taken as unity.

It has been previously established (Longuet-Higgins & Fenton 1974) that M_∞, C_∞, I_∞, T_∞, V_∞, as well as the Froude number of solitary waves, reach maxima for waves below limiting height; the maxima of Froude number, T_∞, V_∞ occur within the range of table 6. In addition, however, the present results are accurate enough to resolve a subsequent minimum, occurring for all variables near $\omega_\infty = 0.995$. A more detailed discussion of this behaviour will be given in §8 for deep-water waves.

The most accurate previous calculations of steep solitary waves are those of Byatt-Smith & Longuet-Higgins (1976) who, by an integral equation technique, covered the range $0.80 \leqslant \omega_\infty \leqslant 0.96$. Within this range their tabulated results have been interpolated for the values of ω_∞ appearing in table 6, and are shown there in parentheses. To the precision of their quoted results, four decimal places for Froude number and three for C_∞, T_∞, V_∞, the agreement is generally excellent.

The highest previous near-limiting solitary waves are due to Sasaki & Murakami (1973), who have published eight solutions in the range $0.984 \leqslant \omega_\infty \leqslant 0.991$, with maximum surface slopes up to 29.9°. For steep waves, the maximum slope has been shown to vary almost linearly with ω_∞ by Longuet-Higgins & Fox (1977), who on this basis demonstrated the consistency of slopes computed by Sasaki & Murakami and Byatt-Smith & Longuet-Higgins (1976). The former results, however, do not quite achieve the present accuracy, as is most evident from their computed crest acceleration, which *falls* from $0.384g$ to $0.379g$ as ω_∞ increases through the above range.

In paper I, (4.26)–(4.28), expressions are given for the error terms arising from p_s in the integral identities derived by Longuet-Higgins (1974) for the solitary wave. Whereas for the limiting solution these errors did not exceed 2×10^{-6}, they now reach values up to 4×10^{-5}, although generally they do not exceed 10^{-5}. It is believed, therefore, that the integral properties of near-limiting solitary waves have been established to four to five decimal places, as presented in table 6. This table also includes interpolated estimates for the maximum Froude number and the value of ω_∞ at which the surface slope first reaches 30°.

8. Deep-water waves

It was shown in paper I that deep-water waves may be deduced, to working accuracy, from the solutions for $d = 10$. Table 7 presents the principal properties of near-limiting deep-water waves computed in this way, with results for the limiting wave, $\omega = 1$, again taken from paper I. These values are based on the normalization of wavelength to 2π and acceleration due to gravity to unity.

Table 7. Properties of limiting and near-limiting deep-water waves

(Values are normalized such that acceleration due to gravity = 1 and wavelength = 2π. Interpolated values giving maximum c and maximum surface slope = 30.00° are shown in italics.)

ω	ϵ'	H/L	c	I	T	V	max. surface slope/deg	y_a
1.00000	0.00000	0.141063	1.092282	0.070113	0.038292	0.034568	30.00	0.60777
0.99924	0.01602	0.141020	1.09227	0.070108	0.038289	0.034566	30.4	0.60776
0.99648	0.03440	0.140867	1.09226	0.070098	0.038283	0.034561	30.3	0.60777
0.99444	0.04327	0.140757	1.09229	0.070094	0.038281	0.034557	30.24	0.60779
0.9858							*30.00*	
0.98396	0.07347	0.140245	1.092488	0.070197	0.038344	0.034606	29.95	0.60806
0.96023	0.11566	0.139179	1.092913	0.070641	0.038602	0.034834	29.29	0.60844
0.9510			*1.092951*					
0.94990	0.12978	0.138707	1.092950	0.070824	0.038704	0.034933	29.01	0.60836
0.94044	0.14146	0.138262	1.092898	0.070965	0.038779	0.035012	28.77	0.60816
0.92976	0.15358	0.137743	1.092748	0.071087	0.038840	0.035084	28.49	0.60781

The tabulated values may be compared with the predictions of Longuet-Higgins & Fox (1978), who by the method outlined in §3 derived (using the above normalization) the following expressions, correct to ϵ'^3:

$$H/L = 0.14107 - 0.50\pi^{-1}\epsilon'^2 + 0.160\epsilon'^3 \cos(2.143 \ln \epsilon' - 1.54), \tag{8.1}$$

$$c^2 = 1.1931 - 1.18\epsilon'^3 \cos(2.143 \ln \epsilon' + 2.22), \tag{8.2}$$

$$I = 0.07011 - 0.364\epsilon'^3 \cos(2.143 \ln \epsilon' + 1.61), \tag{8.3}$$

$$T = 0.03829 - 0.215\epsilon'^3 \cos(2.143 \ln \epsilon' + 1.66), \tag{8.4}$$

$$V = 0.03457 - 0.169\epsilon'^3 \cos(2.143 \ln \epsilon' + 1.49). \tag{8.5}$$

These expressions show that, except for H/L, each variable passes through an infinite succession of maxima and minima in its approach to the limiting value at $\epsilon' = 0$. For $\epsilon' < 0.05$ values of c, I, T, V calculated from (8.2)–(8.5) are compared with values from table 7 in the left-hand part of figure 4. The general trends agree in all cases, with a minimum being shown at $\epsilon' \approx 0.03$

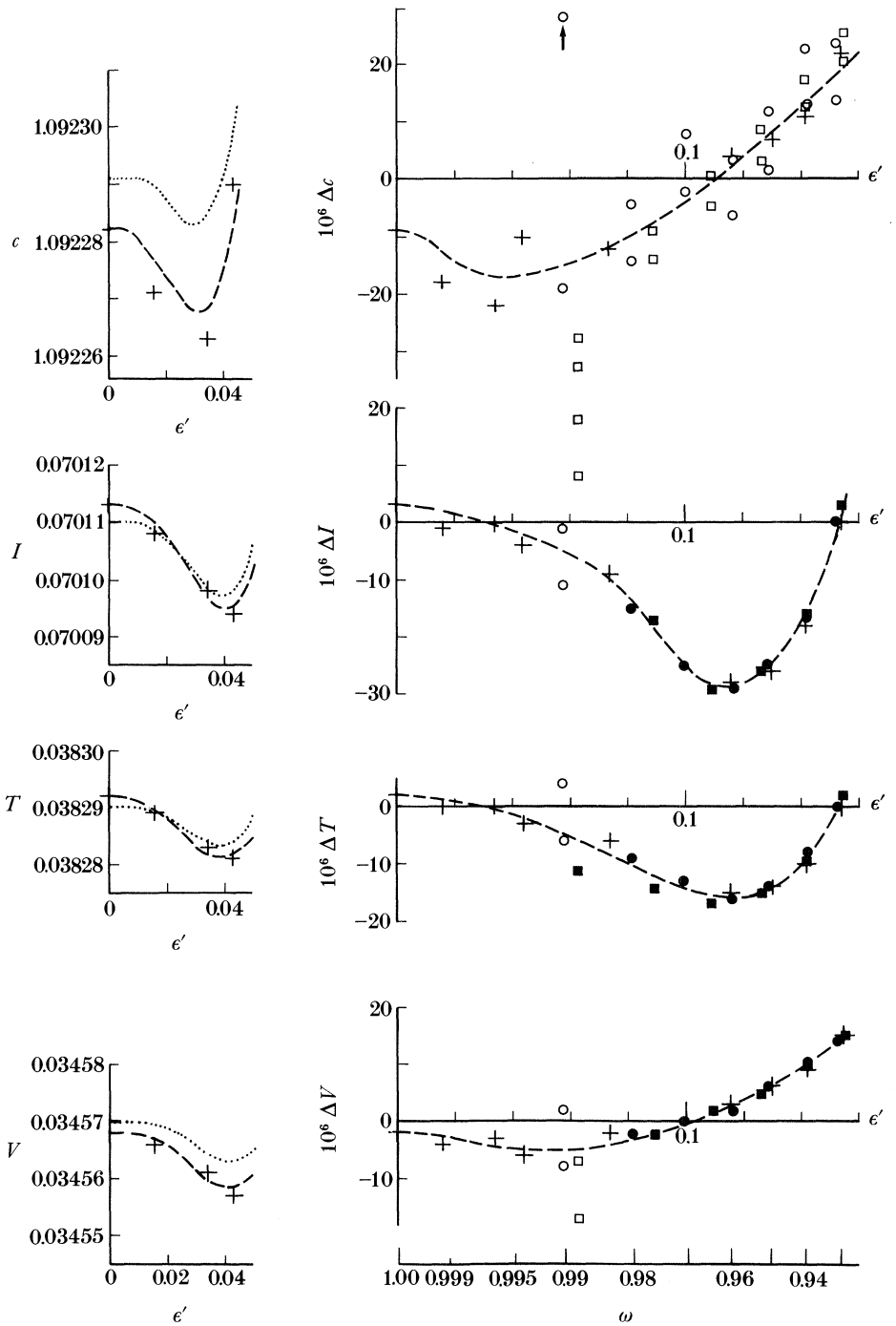

FIGURE 4. The variation of c, I, T, V (left-hand side) and Δc, ΔI, ΔT, ΔV (right-hand side) with ϵ' and ω for deep-water waves; · · · · ·, from (8.2)–(8.5), after Longuet-Higgins & Fox (1978); +, this paper (table 7); ●, Longuet-Higgins (1975), results quoted to six or more decimal places; ○, Longuet-Higgins, range for less than six decimal places; ■, Cokelet (1977), six or more decimal places; □, Cokelet, less than six decimal places; ———, estimated true values, taking all results into account.

PHILOSOPHICAL TRANSACTIONS OF THE ROYAL SOCIETY A MATHEMATICAL, PHYSICAL & ENGINEERING SCIENCES

for c and $\epsilon' \approx 0.04$ for I, T, V. The discrepancy in c would probably be much reduced if Longuet-Higgins & Fox's analysis were repeated with the benefit of the more accurate limiting value found in paper I.

For $\epsilon' > 0.05$, (8.1)–(8.5) are less precise because absent higher-order terms become significant. Nevertheless they provide useful datum functions for investigating the mutual consistency of the present and previous calculations. Therefore, with Δc, ΔI, ΔT, ΔV defined as the difference between a computed result and the value given by (8.2)–(8.5), these differences are plotted against ϵ' in the right-hand part of figure 4; the scale of ω is also shown, at the foot of the diagram. With the present results are included those of Longuet-Higgins (1975) and Cokelet (1977); where these earlier calculations have been quoted to less than six decimal places the implied range is shown on the plot.

Figure 4 shows the mutual consistency of almost all results; only the highest non-limiting solution by Cokelet, for $\omega \approx 0.99$, seems not to justify the number of decimal places quoted. For $\omega < 0.98$ the previous results are probably accurate to five decimal places for c and to within two units in the sixth decimal place for I, T, V. The present results appear to justify quoting generally to six decimal places, with an expected error of up to two units in the last place, except that values of c for $0.99 < \omega < 1.00$ justify only five decimal places. This presentation has been adopted in table 7, which also includes interpolated estimates for maximum c and the first attainment of a 30° surface slope.

Sasaki & Murakami (1973) have also published solutions for very steep deep-water waves, for $0.956 < \omega < 0.974$. The general accuracy approaches that of the present solutions but, as for their solitary waves, the computed crest acceleration decreases with increasing ω.

Angular momentum

Calculations of angular momentum and hence the level of action y_a of near-limiting deep-water waves have been made as described in paper I, which in turn follows the method of Longuet-Higgins (1980). The results are given in the last column of table 7, y_a being measured positively upwards from the mean surface level and normalized relative to a wavelength of 2π.

Although the present solutions are slightly less accurate than for the limiting wave, nevertheless there is a consistency in the sequence of values for y_a suggesting that an accuracy of at least four decimal places and possibly five has been achieved throughout. The reservations on accuracy expressed in paper I may therefore have been overstated.

9. Detailed tabulations

The detailed properties of the flow may be computed from the defining coefficients, such as those of table 2, according to the equations of §11 of paper I. Two cases have been chosen for presentation: with $A = 0.9999$ for $d = 1.0$, 10.0 respectively. For these waves the crest acceleration (table 4) is close to its asymptotic value, the maximum slope exceeds 30°, and the inner profile is large enough in scale to be evident in the tabulation range used in paper I.

Table 8 relates to tables 10*a*–*e* of paper I and shows for $d = 1.0$, $\omega = 0.99612$ (99.83% of limiting height) those parts of the flow field differing significantly from the limiting wave. Displacement is affected only on the surface streamline, while the velocity and acceleration fields show more widespread variations. Time t, taken by a particle from a starting point beneath the wave crest, is also substantially different from the limiting case owing to the absence of the

stagnation point. For each streamline, the increment of time saved in travelling through the crest zone affects the value of t throughout the wavelength, as noted on the table.

Table 9 presents a similar condensed tabulation for $d = 10, \omega = 0.99648$ (99.86% of limiting height), from which the deep-water wave may be derived, and relates to tables 12a–e of paper I. In this case, except for the acceleration field, the tabulations are needed only for the surface streamline, $\psi = 0$.

The surface profiles near the crests of the two waves, for $\phi/\lambda > -0.0002$, are in close agreement, as may be verified by dividing each set of velocities by the relevant scale factor $\sqrt{(l/2F^2)}$; they are approaching the asymptotic form, with computed crest accelerations of $0.3886g$ and $0.3888g$ respectively. Beyond $\phi/\lambda = -0.0003$ the surfaces diverge from the asymptotic profile and begin to merge into the profiles previously computed for the limiting waves.

A special comment is needed on the calculation of $t(\chi)$ for near-limiting waves. The accurate determination of t presents difficulties near the wave crest where velocities are small and time increments consequently large. For limiting waves a series expansion was developed for the surface streamline near the crest, and is described in Appendix 2 of paper I. For near-limiting waves, however, no convenient alternative expansion is available and t has therefore been computed by very fine quadrature for $0 \leqslant \theta/2\pi \leqslant 0.0025$ on the surface streamline.

10. Surface drift velocities

In paper I specimen calculations are presented of particle paths and drift profiles in limiting waves. These show the sharp increase near the surface in the particle advance during a wave cycle, and hence in the drift velocity.

It is of interest to calculate the surface drift velocity for near-limiting waves and determine the rate at which it falls off from its maximum value. Following paper I, (12.1), we calculate the surface drift velocity U_s from

$$U_s = c - L/2t_{(\tau=-1)}. \tag{10.1}$$

Values of U_s/c are given in table 10 and show that, in broad terms, a wave of 99% of maximum height has about 88% of the maximum surface drift velocity, while at 97% of maximum height the drift is about 80% of maximum.

11. Waves of lesser height

The completion of this work on progressive finite-amplitude waves calls for the computation of waves of all lesser heights down to zero, again over the full range of d.

For $A \leqslant 0.985$ both the dipoles and the second leading term of (4.2) may be dispensed with, only a single leading term with a suitable exponent ν being left. The variation of ν with d and A was determined by computing a few trial cases over the full range and finding an empirical fit. A suitable expression was found to be:

$$\nu = 0.230\,373\,497 + 0.051\,288\,646A' - 2.089\,348\,938d' + 0.978\,579\,607A'^2 + 5.584\,276\,399A'd' - 17.986\,307\,552d'^2, \tag{11.1}$$

TABLE 8. FLOW FIELD NEAR THE SURFACE FOR $d = 1.0$, $A = 0.9999$, $\omega = 0.99612$

($1/2F^2 = 0.656518$, $h = 1.94110$, $L = 11.72983$,† $\bar{y}_s = 0.82049$, $l = 0.002034$.
Maximum surface slope = 30.26° (computed), 30.24° (corrected) at $\phi/\lambda = -0.00027$.)

ϕ/λ	0.0000	−0.0001	−0.0002	−0.0005	−0.0010	−0.0015	−0.0025	−0.0050	−0.0100	−0.0175	−0.0250	−0.5000
ψ	horizontal displacement, x											
0.00	0.0000	0.0152	0.0243	0.0448	0.0710	0.0930	0.1308	0.2082	0.3325	0.4870	0.6224	5.8649
	vertical displacement, y											
0.00	−0.0632‡	−0.0569	−0.0517	−0.0398	−0.0246	−0.0121	0.0094	0.0525	0.1195	0.1990	0.2654	1.1437
	horizontal velocity, u											
0.00	0.0517‡	0.0907	0.1152	0.1581	0.2000	0.2294	0.2725	0.3444	0.4354	0.5265	0.5944	1.2599
−0.01	0.2127	0.2131	0.2142	0.2210	0.2384	0.2569	0.2904	0.3542	0.4406	0.5293	0.5961	1.2596
−0.02	0.2673	0.2674	0.2677	0.2701	0.2778	0.2882	0.3116	0.3655	0.4463	0.5323	0.5980	1.2592
−0.03	0.3051	0.3051	0.3053	0.3066	0.3108	0.3171	0.3334	0.3779	0.4525	0.5356	0.5999	1.2589
	vertical velocity, v											
0.00	0.0000	0.0513	0.0670	0.0917	0.1148	0.1307	0.1535	0.1894	0.2301	0.2641	0.2842	0.0000
−0.01	0.0000	0.0088	0.0175	0.0415	0.0727	0.0954	0.1265	0.1715	0.2186	0.2561	0.2778	0.0000
−0.02	0.0000	0.0055	0.0110	0.0270	0.0515	0.0725	0.1050	0.1552	0.2075	0.2482	0.2715	0.0000
	time, t											
0.00	0.0000	0.2297	0.3185	0.4682	0.6146	0.7171	0.8678	1.1187	1.4375	1.7585	2.0002	6.9433
−0.01	0.0000	0.0277	0.0552	0.1336	0.2460	0.3379	0.4819	0.7301	1.0492	1.3713	1.6138	6.5657
−0.02	0.0000	0.0176	0.0351	0.0870	0.1692	0.2441	0.3727	0.6113	0.9279	1.2503	1.4935	6.4538
−0.03	0.0000	0.0135	0.0270	0.0672	0.1326	0.1948	0.3080	0.5331	0.8451	1.1670	1.4106	6.3791
−0.04	0.0000	0.0112	0.0224	0.0559	0.1109	0.1644	0.2647	0.4756	0.7811	1.1018	1.3456	6.3220
−0.05	0.0000	0.0097	0.0194	0.0485	0.0965	0.1436	0.2337	0.4309	0.7288	1.0476	1.2913	6.2754
−0.06	0.0000	0.0087	0.0173	0.0432	0.0861	0.1285	0.2104	0.3951	0.6847	1.0011	1.2446	6.2359
−0.07	0.0000	0.0079	0.0157	0.0392	0.0783	0.1169	0.1923	0.3657	0.6468	0.9602	1.2032	6.2016
−0.08	0.0000	0.0072	0.0144	0.0361	0.0720	0.1077	0.1777	0.3412	0.6136	0.9238	1.1661	6.1713
−0.09	0.0000	0.0067	0.0134	0.0335	0.0670	0.1002	0.1657	0.3205	0.5844	0.8909	1.1324	6.1441
	horizontal acceleration											
0.00	0.0000	0.2660	0.2825	0.2875	0.2860	0.2863	0.2867	0.2862	0.2846	0.2823	0.2795	0.0000
−0.01	0.0000	0.0270	0.0530	0.1190	0.1845	0.2167	0.2450	0.2656	0.2741	0.2759	0.2748	0.0000
−0.02	0.0000	0.0136	0.0270	0.0655	0.1189	0.1573	0.2024	0.2435	0.2630	0.2694	0.2700	0.0000
−0.03	0.0000	0.0090	0.0180	0.0444	0.0847	0.1184	0.1665	0.2213	0.2517	0.2627	0.2651	0.0000
−0.04	0.0000	0.0067	0.0135	0.0334	0.0650	0.0933	0.1386	0.2003	0.2402	0.2559	0.2602	0.0000
−0.05	0.0000	0.0054	0.0107	0.0267	0.0524	0.0764	0.1173	0.1811	0.2287	0.2491	0.2552	0.0000
−0.06	0.0000	0.0045	0.0089	0.0222	0.0438	0.0644	0.1010	0.1640	0.2174	0.2422	0.2503	0.0000
−0.07	0.0000	0.0038	0.0076	0.0190	0.0376	0.0555	0.0882	0.1490	0.2065	0.2354	0.2453	0.0000
−0.08	0.0000	0.0033	0.0066	0.0165	0.0328	0.0486	0.0781	0.1359	0.1960	0.2285	0.2403	0.0000
−0.09	0.0000	0.0029	0.0059	0.0146	0.0291	0.0432	0.0699	0.1245	0.1860	0.2218	0.2353	0.0000
	vertical acceleration											
0.00	0.2551‡	0.1860	0.1715	0.1597	0.1564	0.1539	0.1485	0.1368	0.1177	0.0935	0.0720	−0.0532
−0.01	0.3185	0.3174	0.3142	0.2958	0.2600	0.2333	0.2011	0.1645	0.1316	0.1013	0.0775	−0.0530
−0.02	0.3128	0.3125	0.3116	0.3058	0.2891	0.2698	0.2364	0.1880	0.1444	0.1088	0.0828	−0.0528
−0.03	0.3071	0.3070	0.3066	0.3038	0.2950	0.2829	0.2566	0.2069	0.1562	0.1159	0.0879	−0.0525
−0.04	0.3018	0.3017	0.3015	0.2999	0.2945	0.2866	0.2670	0.2211	0.1666	0.1226	0.0928	−0.0523
−0.05	0.2967	0.2967	0.2965	0.2955	0.2919	0.2864	0.2717	0.2315	0.1758	0.1289	0.0975	−0.0521
−0.06	0.2920	0.2919	0.2918	0.2911	0.2885	0.2845	0.2732	0.2386	0.1838	0.1347	0.1019	−0.0519
−0.07	0.2874	0.2874	0.2873	0.2867	0.2848	0.2818	0.2729	0.2433	0.1906	0.1401	0.1062	−0.0516
−0.08	0.2830	0.2830	0.2829	0.2825	0.2810	0.2786	0.2715	0.2462	0.1962	0.1451	0.1102	−0.0514
−0.09	0.2788	0.2788	0.2787	0.2784	0.2772	0.2753	0.2694	0.2477	0.2008	0.1496	0.1139	−0.0512
−0.10	0.2747	0.2747	0.2747	0.2744	0.2734	0.2718	0.2670	0.2482	0.2045	0.1536	0.1174	−0.0510

† $\bar{y}_s$ = average value of y on the surface.

In general, tables 10*a–e* of paper I define also the flow field of this wave with a discrepancy not exceeding 0.0002. The exceptions, for tables 10*c*, *d*, are tabulated above, with the origin values, marked ‡, applying also to tables 10*a*, *b*. Table 10*b* also needs the following adjustments:

Time t: for $\psi = 0$, $\phi/\lambda = -0.05(-0.05)-0.50$, reduce by 0.0922.

PHILOSOPHICAL TRANSACTIONS OF THE ROYAL SOCIETY A MATHEMATICAL, PHYSICAL & ENGINEERING SCIENCES

TABLE 9. FLOW FIELD NEAR THE SURFACE FOR $d = 10.0$, $A = 0.9999$, $\omega = 0.99648$

($1/2F^2 = 5.000000$, $h = 1.89783$, $L = 1.18484$, $\dagger \bar{y}_s = 0.20217$, $l = 0.000223$.
Maximum surface slope = 30.30° (computed), 30.29° (corrected) at $\phi/\lambda = -0.00028$.)

ϕ/λ	0.0000	−0.0001	−0.0002	−0.0005	−0.0010	−0.0015	−0.0025	−0.0050	−0.0100	−0.0175	−0.0250	−0.5000
ψ	horizontal displacement, x											
0.00	0.0000	0.0017	0.0027	0.0049	0.0078	0.0102	0.0143	0.0227	0.0362	0.0528	0.0674	0.5924
	vertical displacement, y											
0.00	0.0899‡	0.0906	0.0912	0.0925	0.0941	0.0955	0.0979	0.1026	0.1101	0.1191	0.1266	0.2568
	horizontal velocity, u											
0.00	0.0472‡	0.0828	0.1052	0.1443	0.1826	0.2093	0.2486	0.3140	0.3965	0.4790	0.5405	1.2928
	vertical velocity, v											
0.00	0.0000	0.0468	0.0613	0.0840	0.1054	0.1202	0.1416	0.1760	0.2168	0.2537	0.2782	0.0000
	time, t											
0.00	0.0000	0.0275	0.0382	0.0561	0.0736	0.0859	0.1039	0.1339	0.1718	0.2099	0.2383	0.7577
	horizontal acceleration											
0.00	0.0000	2.0250	2.1508	2.1918	2.1783	2.1783	2.1811	2.1800	2.1726	2.1649	2.1583	0.0000
−0.01	0.0000	0.0204	0.0408	0.1019	0.2028	0.3018	0.4910	0.8901	1.3734	1.6801	1.8094	0.0000
−0.02	0.0000	0.0099	0.0199	0.0497	0.0993	0.1487	0.2462	0.4785	0.8670	1.2494	1.4674	0.0000
−0.03	0.0000	0.0065	0.0129	0.0324	0.0647	0.0969	0.1611	0.3179	0.6054	0.9467	1.1845	0.0000
	vertical acceleration											
0.00	1.9438‡	1.4197	1.3097	1.2313	1.2110	1.2007	1.1763	1.1197	1.0272	0.9100	0.8041	−1.5056
−0.01	2.2413	2.2412	2.2409	2.2389	2.2318	2.2202	2.1849	2.0491	1.7401	1.3965	1.1651	−1.4405
−0.02	2.0623	2.0622	2.0622	2.0616	2.0598	2.0566	2.0468	2.0029	1.8588	1.6031	1.3738	−1.3781
−0.03	1.9127	1.9127	1.9127	1.9124	1.9116	1.9101	1.9055	1.8844	1.8077	1.6411	1.4587	−1.3180

† $\bar{y}_s$ = average value of y on the surface.

In general, tables 12*a–e* of paper I define also the flow field of this wave with a discrepancy not exceeding 0.0002. The exceptions, for tables 12*c*, *d*, are tabulated above, with the origin values, marked ‡, applying also to tables 12*a*, *b*. Table 12*b* also needs the following adjustments:

Time, t: for $\psi = 0$, $\phi/\lambda = -0.05(-0.05)-0.50$, reduce by 0.0111.

Horizontal acceleration: for $\psi = 0$, $\phi/\lambda = -0.10$, reduce by 0.0003.

Vertical acceleration: for $\psi = 0$, $\phi/\lambda = -0.05$, -0.10, increase by 0.0003.

TABLE 10. DRIFT VELOCITIES AT THE SURFACE

(Tabulated values are of the ratio of surface drift velocity to celerity, U_s/c.)

d	0.2	0.5	1.0	2.0	10.0
A					
1.0	0.0774	0.1531	0.2219	0.2656	0.2734
0.99999	0.0742	0.1488	0.2171	0.2607	0.2685
0.9999	0.0707	0.1438	0.2115	0.2550	0.2628
0.999	0.0634	0.1334	0.1997	0.2428	0.2506
0.99	0.0471	0.1106	0.1740	0.2164	0.2240

where
$$A' = 0.45 + 0.2122 \exp\left[-4.551(1-A)^{\frac{1}{3}}\right], \tag{11.2}$$

and
$$d' = 0.005 - R^{1.917}/29.964. \tag{11.3}$$

Table 11 shows some specimen values of ν (rounded to four decimal places) evaluated in this way, with the ratio $H/H_{\max}$ of the resulting wave. We note that all values of ν are close to, but many are less than, $\frac{1}{2}$.

Table 11. Exponent of leading term for waves of lesser height, as given by (11.1)–(11.3)

(Upper tabulated values are of ν (equation (4.2)), lower values $H/H_{\max}$.)

d	0.2	0.5	1.0	2.0	10.0
A					
0.985	0.5006	0.5133	0.5207	0.5238	0.5243
	0.8782	0.9377	0.9595	0.9673	0.9683
0.95	0.4730	0.4840	0.4902	0.4926	0.4929
	0.7104	0.8472	0.9007	0.9190	0.9215
0.90	0.4605	0.4707	0.4762	0.4783	0.4786
	0.5543	0.7444	0.8280	0.8568	0.8607
0.80	—	0.4606	0.4657	0.4675	0.4677
	—	0.5873	0.7023	0.7431	0.7485
0.70	—	—	0.4612	0.4628	0.4631
	—	—	0.5927	0.6381	0.6443
0.60	—	—	—	—	0.4605
	—	—	—	—	0.5452

For waves below about 60 % of maximum height the leading term also was discarded, leaving only the sequence ζ_m as originally described in §5 of paper I.

Numerous tables of waves computed in this way are presented in the author's Ph.D. thesis (Williams 1983).

12. Discussion

The results presented in this paper include the first fully detailed solutions of non-breaking waves having slopes exceeding 30°. The general accuracy, although a little short of that achieved for limiting waves in paper I, is greater than has been obtained in previous work on steep waves, with the exception of the solution by Longuet-Higgins & Fox (1977) of the asymptotic inner profile. The present work successfully demonstrates the approach of the crest profiles to the asymptotic form, despite their very small scale, and supports Longuet-Higgins & Fox's estimate of the asymptotic maximum slope of 30.37° (possibly 30.38°) and crest acceleration of $0.388g$.

As with the limiting wave solutions of paper I, the results have been shown to be consistent with previous work on steep solitary and deep-water waves. In particular, the accuracy is sufficient to resolve not only the well-known first maximum of celerity and other quantities but also the next minimum in the expected infinite sequence. It is noteworthy that this minimum has been identified without specific inclusion of the terms with complex exponent in (3.4). These terms express the oscillatory asymptotic behaviour of the inner profile, which leads, as demonstrated by Longuet-Higgins & Fox (1978), to the oscillatory behaviour of the wave properties. The present work therefore provides a stringent independent verification of their results.

The results, together with those of paper I, should provide useful data in support of theoretical analysis of the still unsolved question of the position and nature of the singularities in limiting and near-limiting waves. In the field of practical numerical methods the work has also demonstrated the feasibility of resolving accurately features of greatly differing scale; this should be relevant to a wide range of problems, not only of fluid flow, involving near-singular behaviour.

This work formed part of the research programme of the Hydraulics Research Station, now Hydraulics Research Ltd. It is published with the permission of the Managing Director, Dr T. J. Weare, to whom the author is much indebted for his continued encouragement. The keen interest of Professor M. S. Longuet-Higgins, F.R.S., of Cambridge University is also gratefully acknowledged. The computations were done at the University of London Computer Centre through the Institute of Computational Mathematics, Brunel University, where the author was registered for a Ph.D. degree. It is again a pleasure to thank the staff of U.L.C.C. for their invaluable services.

References

Byatt-Smith, J. G. B. & Longuet-Higgins, M. S. 1976 *Proc. R. Soc. Lond.* A **350**, 175–189.
Chen, B. & Saffman, P. G. 1980 *Stud. appl. Math.* **62**, 1–21.
Cokelet, E. D. 1977 *Phil. Trans. R. Soc. Lond.* A **286**, 183–230.
Grant, M. A. 1973 *J. Fluid Mech.* **59**, 257–262.
Lamb, H. 1932 *Hydrodynamics* (6th edn), §229. Cambridge University Press.
Longuet-Higgins, M. S. 1974 *Proc. R. Soc. Lond.* A **337**, 1–13.
Longuet-Higgins, M. S. 1975 *Proc. R. Soc. Lond.* A **342**, 157–174.
Longuet-Higgins, M. S. 1980 *J. Fluid Mech.* **97**, 1–25.
Longuet-Higgins, M. S. & Fenton, J. D. 1974 *Proc. R. Soc. Lond.* A **340**, 471–493.
Longuet-Higgins, M. S. & Fox, M. J. H. 1977 *J. Fluid Mech.* **80**, 721–741.
Longuet-Higgins, M. S. & Fox, M. J. H. 1978 *J. Fluid Mech.* **85**, 769–786.
Olfe, D. B. & Rottman, J. W. 1980 *J. Fluid Mech.* **100**, 801–810.
Sasaki, K. & Murakami, T. 1973 *J. oceanogr. Soc. Japan* **29**, 94–105.
Schwartz, L. W. 1974 *J. Fluid Mech.* **62**, 553–578.
Stokes, G. G. 1880 *Mathematical and physical papers*, vol. 1, pp. 225–228. Cambridge University Press.
Williams, J. M. 1981 *Phil. Trans. R. Soc. Lond.* A **302**, 139–188. (Paper I.)
Williams, J. M. 1983 Ph.D. thesis, Brunel University.

Erratum to paper I

On p. 159 the passage beginning in the fifth line from the bottom of the main text should read:

'...the corrections to be applied to the last three of the above quantities are of order -0.0003, -0.0001, -0.0012 respectively.'

PHILOSOPHICAL TRANSACTIONS OF THE ROYAL SOCIETY A MATHEMATICAL, PHYSICAL & ENGINEERING SCIENCES